A comparison of the fracture mechanics models for the current analyses and the conventional method are summarized in Table 11. The comparison shows that the models used in the current analyses would provide a higher estimate for the SIF. The net result would be a higher crack growth rate and hence a larger crack propagation length for one (1) cycle of operation. These improvements in analysis methods are believed to more accurately predict crack behavior in the CEDM configuration and may be conservative compared to the conventional approach.

Table 11 Comparison of Fracture Mechanics Models

Flaw Type	Feature	Conventional Approach	Entergy Approach
Surface Flaws (ID & OD) Part Throughwall	Stress	Distribution Fixed a Initial flaw Location	Variable Distribution along Length of Tube & Flaw face Pressurized
	Cylinder Geometry	Fixed "R/t" ratio of 4.0	Variable "R/t" ratio from 1 to 300
	Flaw Geometry	Fixed Aspect Ratio; "a/c" = 0.33	Variable Aspect Ratio; "a/c" from 0.2 to 1.0
	Flaw Growth	Only Growth in Depth direction Evaluated	Growth both in the Depth and Length directions evaluated Independently
Throughwall Axial Flaws	Stress	Uniform Tension @ Initial flaw Location	Variable along Length; Both Membrane and Bending components considered; Flaw face Pressurized
	Model	Center Cracked Panel without Correction Factors	Thick Cylinder with correction for Flaw/Tube geometry

Results

Analysis for the As-Built Condition

The first set of analyses was performed using the as-built dimensions for the welds which were estimated from the review of the Plant A UT data. In addition, these analyses were performed by setting the blind zone elevation at 1.544 inches above the nozzle bottom. These analyses were performed at three azimuthal locations on the nozzle (downhill, mid-plane, and uphill). At each location, three crack geometries (ID surface, OD surface, and through-wall) were evaluated. The extent of the compression zone in each nozzle group at the three locations was obtained from the stress distributions presented in Figures 8-17. From these figures, the compression zone at the three azimuthal locations is presented in Table 12, below. In these regions of compression, no PWSCC-assisted crack growth is possible; therefore, these zones can be excluded from consideration for inspection. For those nozzle groups with tensile stress below 10 ksi the possibility for PWSCC crack initiation is

extremely low. The region showing a high hoop tensile stress, (49.7° nozzle at mid-plane), was selected for additional fracture mechanics analysis.

Table 12: Results for Compression Zone

Nozzle Group Head Angle (Degrees)	Azimuthal Location	Height of Compression Zone (inch) (Measured from Nozzle Bottom)	Comment
0	All (360°)	0.89	
7.8	Downhill	0.97	
	Uphill	1.26	
	Mid-Plane	1.059	
29.1	Downhill	1.148	
	Uphill	0	OD Tension {1.66 ksi}
	Mid-Plane	0	ID Tension {6.95 ksi}
49.7	Downhill	0	OD Tension {2.32 ksi}
	Uphill	0	OD Tension {6.11 ksi}
	Mid-Plane	0	ID Tension {19.02 ksi}

All nozzles at the three principal locations (downhill, uphill and mid-plane) showed a measurable freespan length to exist. For these nozzles the three configurations; ID and OD surface and through-wall axial cracks were evaluated.

Thirty (30) analyses cases were performed. The worksheets representing these evaluations are presented in Appendix C, Attachments 1 - 30. The results from this set of analyses are summarized in Table 13. Table 13 provides the "Propagation Dimension" which represents the available freespan for the limiting nozzle within the specific nozzle group. For the surface Crack Type, the length dimension excludes the 0.16 inches that was assumed for the portion of the crack that extends into the freespan.

Table 13 also provides "Growth/Cycle" dimensions. This is the calculated crack growth for one cycle of operation and is used to evaluate the available propagation dimension of each individual nozzle (as determined from the UT data). This is done by comparing the available nozzle propagation dimension to the "Growth/Cycle" dimension. Where the available propagation dimension is larger, adequate margin for flaw growth is available without compromising the weld. When comparing the OD surface crack, 0.16 inch is subtracted from the available propagation dimension to account for the portion of the assumed crack that extends into the freespan.

The analysis results indicate that the OD surface or the through-wall axial crack configurations are not susceptible to crack growth by PWSCC. The analyses show

that the prevailing stresses at the crack location produce a SIF which is below the threshold value. Hence, the potential for crack growth due to PWSCC does not exist.

None of the postulated ID part through-wall cracks came close to reaching the bottom of the weld or penetrating through the wall to meet the weld. Only in two of the cases evaluated (0° nozzle and 7.8° nozzle at the downhill location) did the analysis indicate potential for PWSCC crack growth. In both cases the estimated growth for one cycle of operation was well within the acceptable limits. Hence, there is no evidence to support that an ID initiated part through-wall crack would provide a leak path or reach the weld within one operating cycle.

In all thirty (30) cases evaluated for cracks postulated at the blind zone, the results demonstrate that a postulated flaw in the blind zone region will not compromise the weld in one cycle of operation. The analysis further demonstrates that a larger margin exists (longer than one fuel cycle) at all the plausible locations evaluated.

One nozzle location (49.7° nozzle at mid-plane) showed tensile stress of 19.02 ksi to exist on the ID surface at the nozzle bottom (Figure 17 and Table 10). The nozzle at this location was analyzed to ascertain the behavior of a postulated crack in this region. The analysis performed and the results obtained are discussed in the following subsection (Additional Analysis) for the 49.7° nozzle.

Table 13: WSES-3 Estimated As-Built Analyses Results Summary

Nozzle Angle (Reactor Vessel Head)	Azimuth Location	Crack Type	Fracture Mechanics Results		Attachment Number in Appendix C
			Propagation Dimension (L= length; D= depth) (inch)	Growth / Cycle (inch)	
0 Degree	All	ID	0.869L/0.661D*	*.032L/.064D* *	1
		OD	0.869	0	2
		TW	1.029	0	3
7.8 Degree	Downhill	ID	0.842L/0.661D*	*.022L/.056D* *	4
		OD	0.842	0	5
		TW	1.002	0	6
	Uphill	ID	1.496/0.661D*	*0 L/0 D* *	7
		OD	1.496	0	8
		TW	1.656	0	9
	Mid-Plane	ID	1.169L/0.661D*	*0 L/0 D* *	10
		OD	1.169	0	11
		TW	1.329	0	12
29.1 Degree	Downhill	ID	0.477L/0.661*	*0 L/0 D* *	13
		OD	0.477	0	14
		TW	0.637	0	15
	Uphill	ID	3.456L/0.661D*	*0 L/0 D* *	16
		OD	3.456	0	17
		TW	3.616	0	18
	Mid-Plane	ID	1.981L/0.661D*	*0 L/0 D* *	19
		OD	1.981	0	20
		TW	2.141	0	21
49.7 Degree	Downhill	ID	0.26L/0.661D*	*0 L/0 D* *	22
		OD	0.26	0	23
		TW	0.42	0	24
	Uphill	ID	6.147L/0.661D*	*0 L/0 D* *	25
		OD	6.147	0	26
		TW	6.307	0	27
	Mid-Plane	ID	3.281L/0.661D*	*0 L/0 D* *	28
		OD	3.281	0	29
		TW	3.441	0	30

*For ID Surface Cracks the dimensions for both in Length (L) and Depth (D) are provided.

The graphical presentation of results for those nozzle groups which showed insufficient propagation length are discussed below, by nozzle group. In the graph for length growth, a vertical red line represents one fuel cycle and a horizontal blue line represents available propagation length. When the curve is below the intersection point of these two lines, the analysis indicates that the postulated crack will not reach the bottom of the weld in one operating cycle. In addition graphs for the through-wall cracks for all nozzle groups at the downhill location, which has the smallest available propagation length, are provided. Since the through-wall cracks are the limiting configuration, the absence of crack growth demonstrates that there exists sufficient margin to preclude PWSCC growth from compromising the weld.

0° Nozzle

In this nozzle the ID surface crack showed potential for PWSCC assisted crack growth. The crack growth and the corresponding SIF are presented in Figure 24. The plots show that the crack growth is very small and significantly lower than the limiting condition that would compromise the weld. The graph for the through-wall crack, Figure 25, shows that a through-wall crack postulated at the blind zone shows no crack growth. The SIF for this crack is below the threshold value required for crack growth.

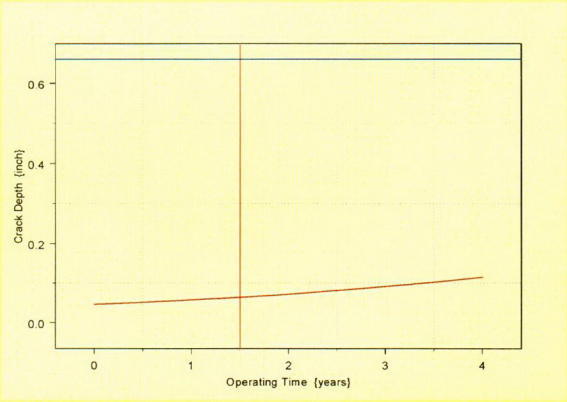

{Depth Growth}

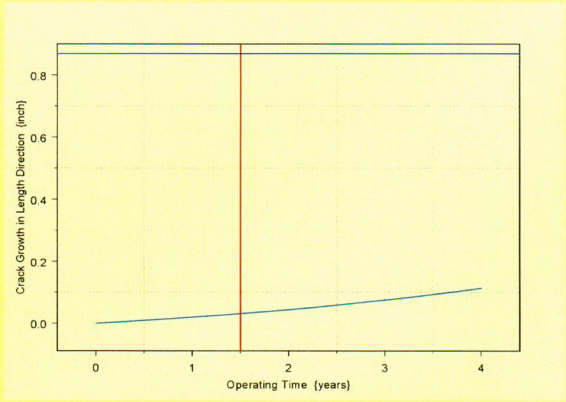

{Length Growth}

Figure 24: *Nozzle at 0° ID Surface Crack. Crack growth in both the depth and length are shown. In both cases the crack growth is well below the intersection of the red and blue lines indicating sufficient margin. The SIF plot shows the SIF at both the depth (a-tip) and surface (c-tip) points. Note the surface point SIF is higher than the depth point SIF indicating that the crack growth would be more pronounced along the surface*

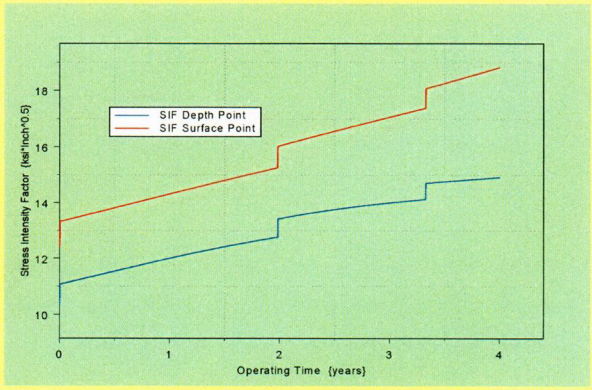

{SIF}

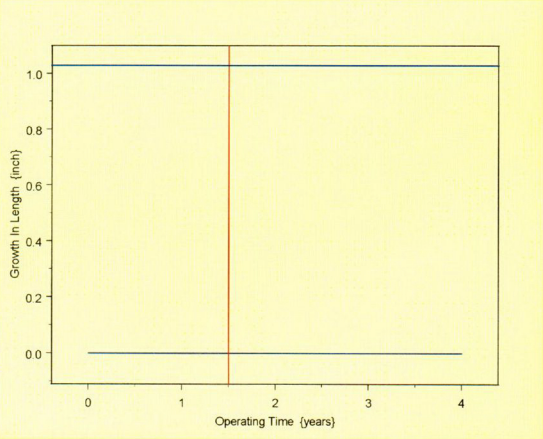

{Growth}

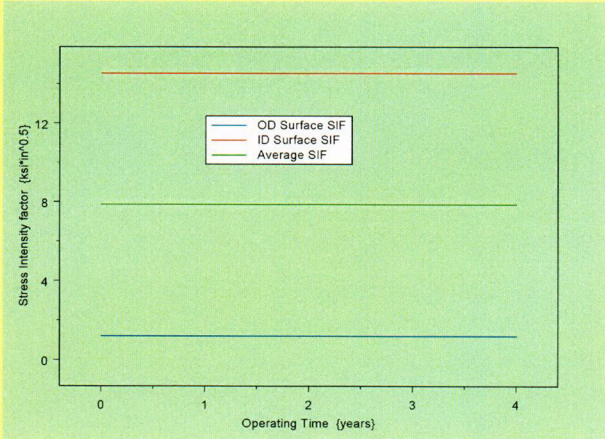

{SIF}

Figure 25: *Nozzle at 0° through-wall crack. No crack growth is observed. The SIF plot shows that the average SIF is below the threshold value of 8.19 ksi√in.*

C09

7.8° Nozzle Group

In this nozzle the ID surface crack showed potential for PWSCC assisted crack growth. The crack growth and the corresponding SIF are presented in Figure 26. The plots show that the crack growth is very small and significantly lower than the limiting condition that would compromise the weld. The graph for the through-wall crack, Figure 27, shows that a through-wall crack postulated at the blind zone shows no crack growth. The SIF for this crack is below the threshold value required for crack growth.

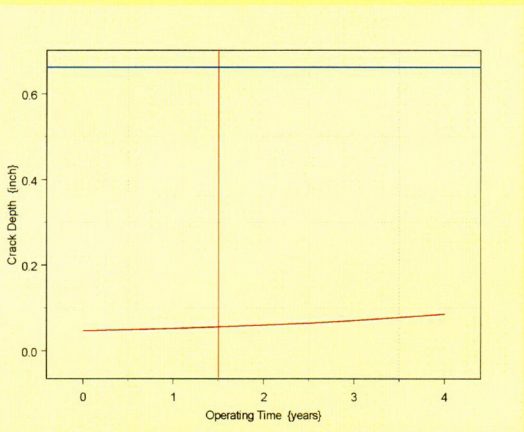

{Depth Direction}

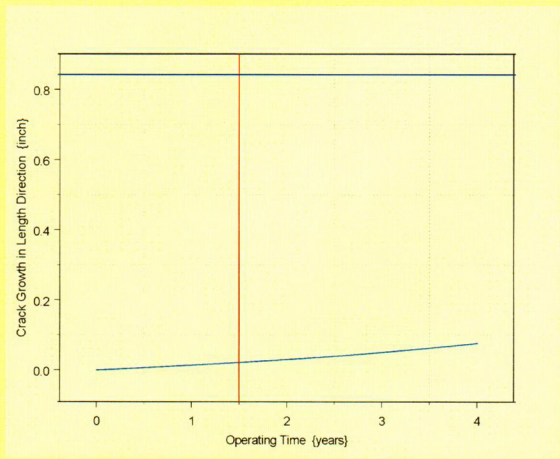

{Length Direction}

Figure 26: *Nozzle at 7.8° ID Surface Crack. Crack growth in both the depth and length are shown. In both cases the crack growth is well below the intersection of the red and blue lines indicating sufficient margin. The SIF plot shows the SI at both the depth (a-tip) and surface (c-tip) points. Note the surface point SIF is higher than the depth point SIF indicating that the crack growth would be more pronounced along the surface*

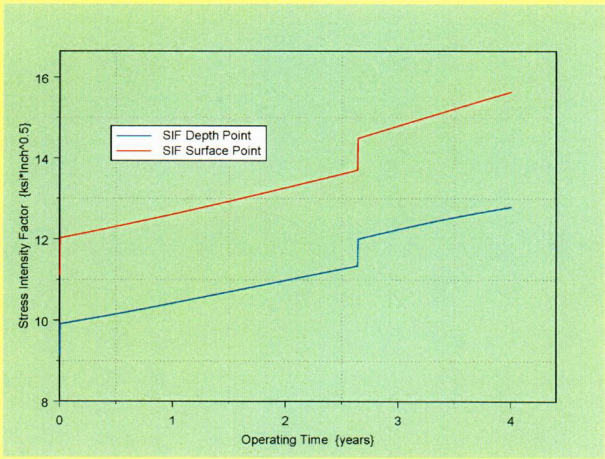

{SIF}

C10

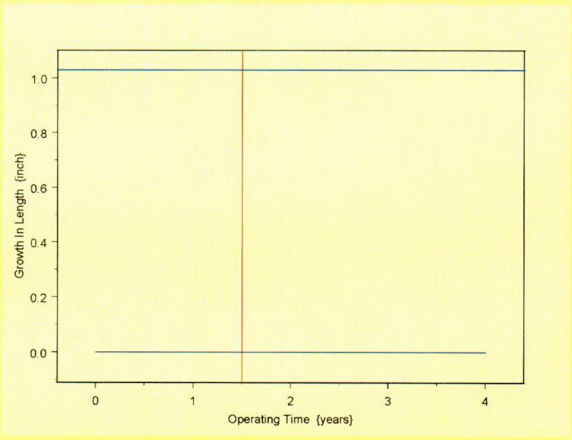

{Crack Growth}

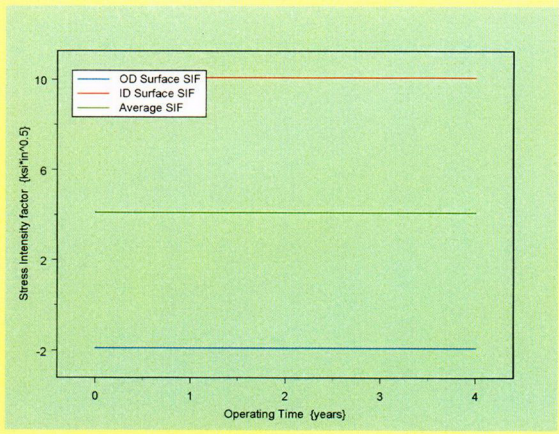

{SIF}

Figure 27: *Nozzle at 7.8° through-wall crack. No crack growth is observed. The SIF plot shows that the average SIF is below the threshold value of 8.19 ksi√in.*

29.1° Nozzle Group

The results for this nozzle group showed no potential for crack growth at all locations and the three crack configurations evaluated. The results for the through-wall crack at the downhill location are presented in Figure 28 below.

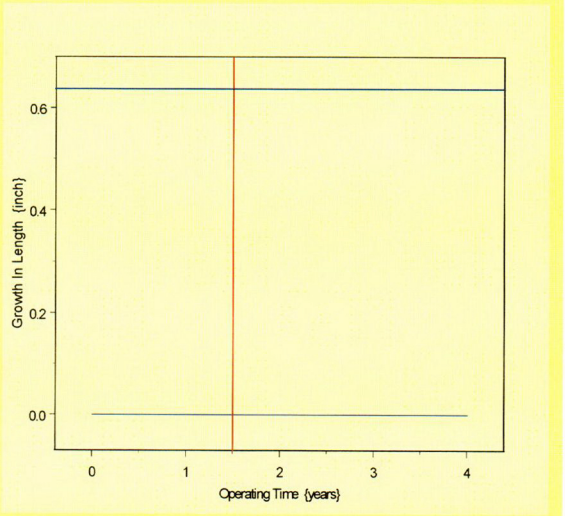

{Crack Growth}

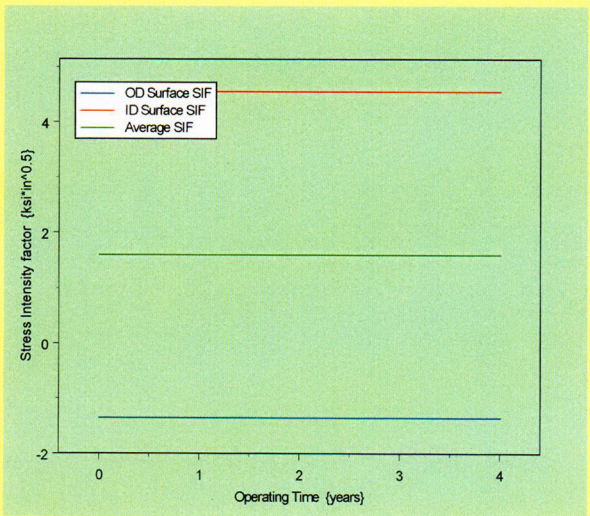

{SIF}

Figure 28: *Nozzle at 29.1° through-wall crack. No crack growth is observed. The SIF plot shows that the average SIF is below the threshold value of 8.19 ksi√in.*

C11

49.7° Nozzle Group

The results for this nozzle group showed no potential for crack growth at all locations and the three crack configurations evaluated. The results for the through-wall crack at the downhill location are presented in Figure 29 below.

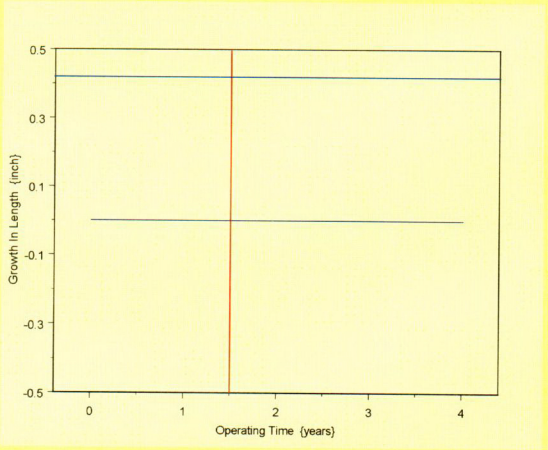

{Crack Growth}

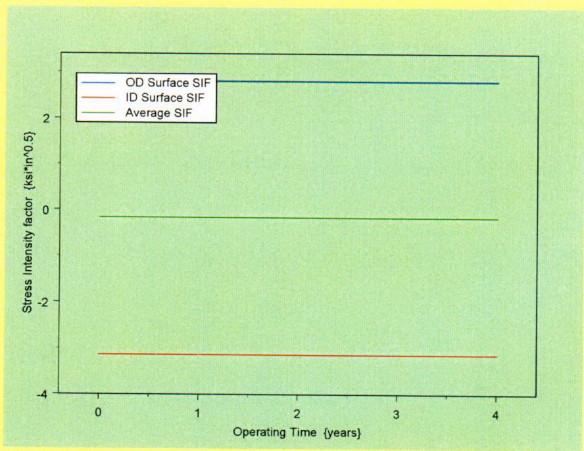

{SIF}

Figure 29: : *Nozzle at 49.7° through-wall crack. No crack growth is observed. The SIF plot shows that the average SIF is below the threshold value of 8.19 ksi√in.*

Additional Analysis

In nozzle group at 49.7° it was determined that the ID stress at the nozzle bottom was about 19.02 ksi. The stress distribution in the region immediately above the nozzle bottom up to the weld bottom was reviewed. Figure 30 presents the stress distribution in this region for the ID surface, the mid-wall, and the OD surface. These distributions were obtained from the regression analyses presented in Attachment 6 of Appendix D. The stress distribution shows that the hoop stress on the ID surface is rapidly decaying to zero and that the distributions at the mid-wall and OD surface show compressive stresses in the immediate vicinity. Therefore it is unlikely that a through-wall edge crack can be supported by the prevailing stress distribution. However, the close proximity of the nozzle bottom necessitates a fracture mechanics analysis using an edge crack formulation in addition to the ID surface crack evaluation. Therefore, three crack configurations were evaluated for this location. Two crack sizes for the ID surface crack geometry and one edge crack geometry were used. The analysis results for these cases are presented in Attachments 31 through 33 of Appendix C, a graphical display of the results are presented and discussed in the following pages.

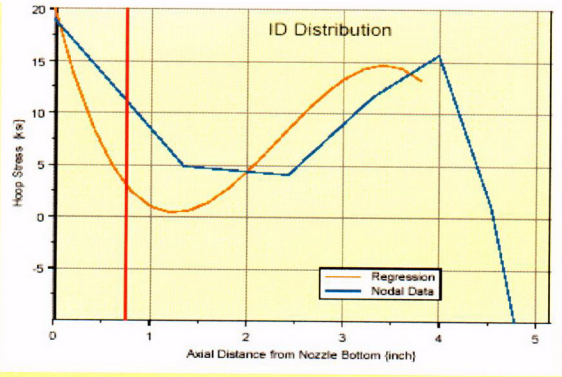

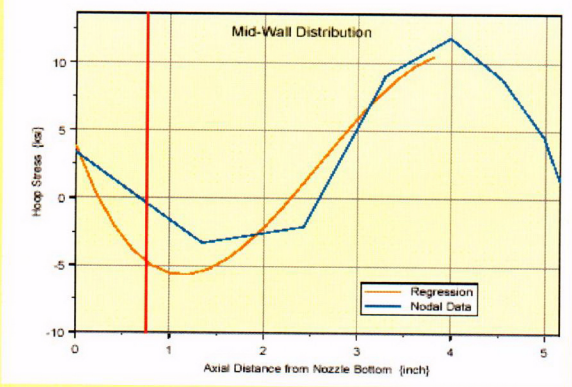

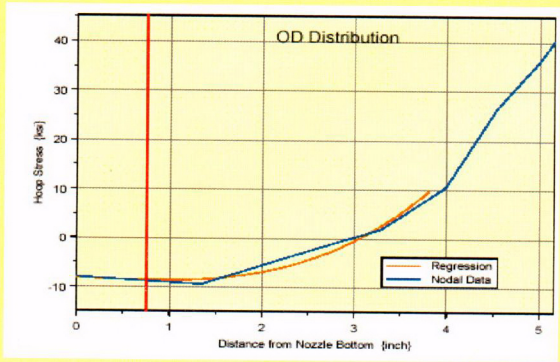

Figure 30: *Nozzle 49.7° at mid-plane location. Hoop stress distribution near nozzle bottom at the ID surface, mid-wall, and OD surface. The vertical red line is set at 0.75 inch from the nozzle bottom. Though the ID surface at the nozzle bottom has a tensile stress of 19.02 ksi, the stress decays rapidly to zero within a short distance. Whereas the stresses at the mid-wall and OD surface are compressive in this region.*

Two ID surface cracks were postulated close to the nozzle bottom. The first crack, with similar dimensions to those considered here was located close (crack center 0.5 inch above nozzle bottom) to the nozzle bottom. The fracture mechanics evaluation (Mathcad worksheet) is presented in Attachment 31 of Appendix C. The graphical results from this analysis are presented in Figure 31. These results show that the postulated crack will not grow by PWSCC. The second crack configuration, a larger ID surface crack which had a depth of 0.33 inch (50% TW) and 0.75 inch long (based on the axial distribution of the hoop stress) was evaluated. The fracture mechanics evaluation (Mathcad worksheet) is presented in Attachment 32 of Appendix C. The results are graphically shown in Figure 32. Once again these results show that there is no potential for crack growth.

Since the location of the postulated crack was so close to the free end of the nozzle and the fracture mechanics models were for cracks removed from the edge, an edge crack model was evaluated to ensure that the results from the ID surface analysis could be supported. The edge crack model was the same model used in the comparison study presented in Attachment 3 of Appendix D. The Mathcad formulation and the analysis are presented in Attachment 33 of Appendix C. The results from this analysis are presented in Figure 33. The initial flaw length was 0.75 inch (based on the stress distribution) and the plate height was set at 4.985 inches (bottom of weld). In this configuration the limiting flaw size, to maintain the validity of

SICF (i.e. Crack Length/Plate Height $\leq$ 0.6), was 2.99 inches. The results show that the postulated crack does not reach the weld in forty (40) years of operation. Though the stress distribution does not favor a through-wall edge crack configuration, this crack configuration would provide the limiting case if the limit of the crack length to plate height ratio remained below 0.6. In the analysis presented in Attachment 33 of Appendix C, the crack length of 2.99 inch (that is; 0.6 x 4.985) is reached in about thirty nine (39) years. This limit is well below the bottom of weld elevation. The results from this analysis are extremely conservative because the initial through-wall crack is not likely to form. However, this analysis does show that the localized region at the bottom of the nozzle would not be cause for concern. Therefore not inspecting this region will not (negatively) impact the level of quality or safety.

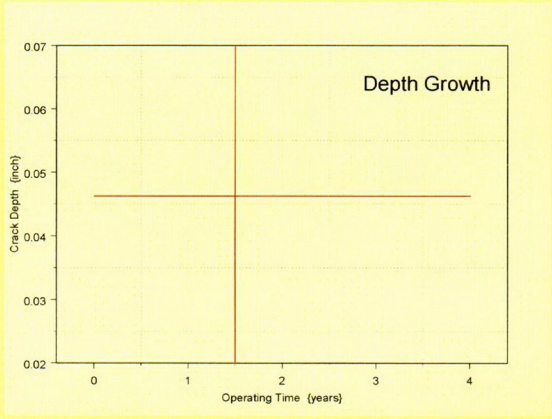

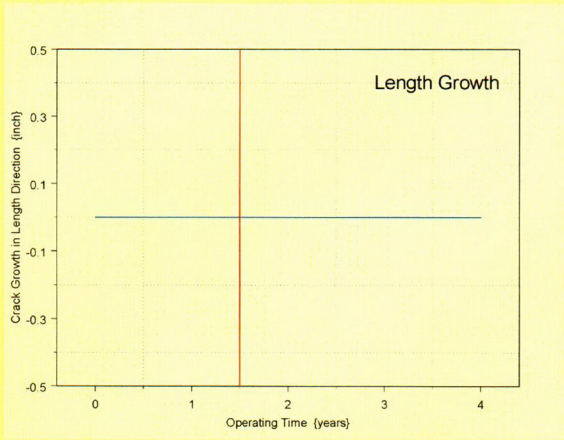

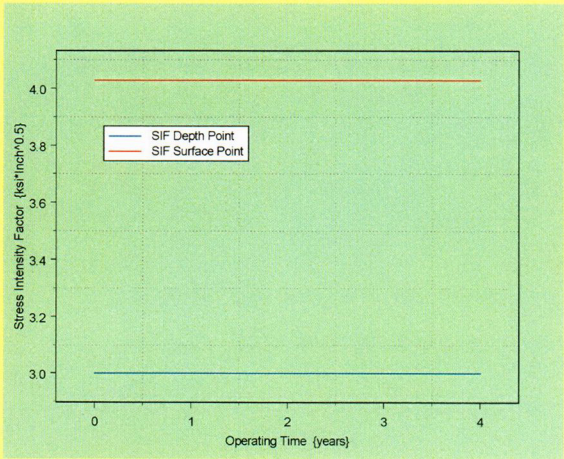

Figure 31: *Nozzle 49.7° at mid-plane location ID surface crack. The crack dimensions are similar to that used for the as-built analysis at the blind zone location. The crack was placed close to the nozzle bottom. The fracture mechanics results demonstrate that this ID surface crack will not grow by a PWSCC mechanism.*

{SIF}

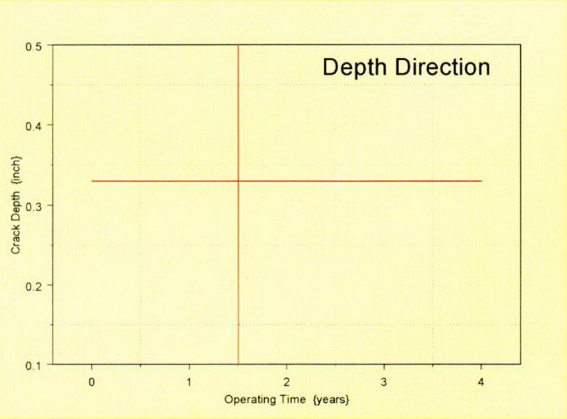

Figure 32: *Nozzle 49.7° at mid-plane location with a larger ID surface crack. The crack dimensions are larger than that used for the as-built analysis at the blind zone location. The crack depth was 0.33 inch and the length was 0.75 inch. The crack was placed close to the nozzle bottom. The fracture mechanics results demonstrate that this ID surface crack will not grow by a PWSCC mechanism.*

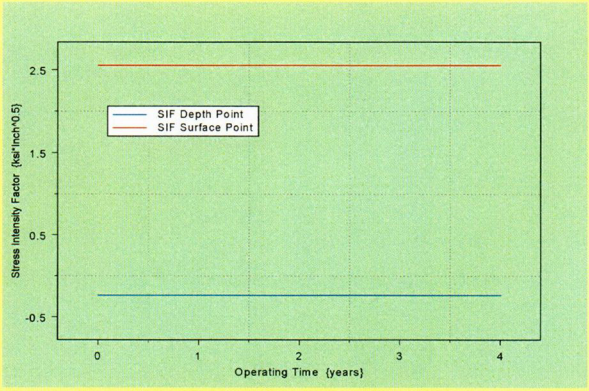

{SIF}

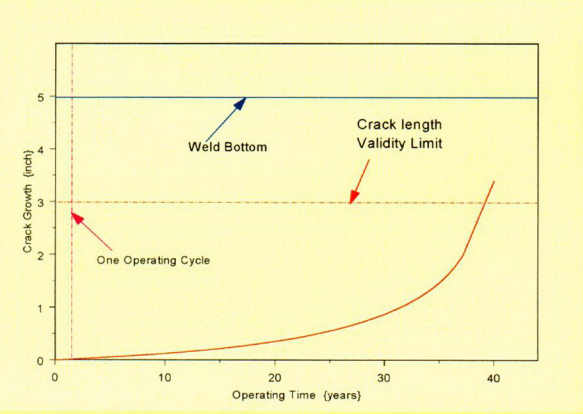

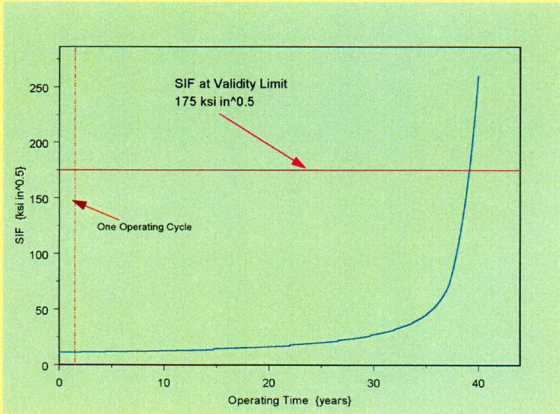

Figure 33: *Nozzle 49.7° at mid-plane location with an edge crack. The estimated crack growth does not cause the initial postulated crack to reach weld bottom in forty (40) years. The SIF at the validity limit is 175 ksi√in., which is significantly higher than the asymptotic maximum for crack growth. Hence the crack growth rate would be about 0.5 inch per year after thirty five (35) years (knee in the curve).*

6.0 Conclusions

The evaluation performed and presented in the preceding sections support the following conclusions:

1) The detailed deterministic analyses incorporating the as-built dimensions for the weld and nozzle length were used to accurately define the inspection zones for the CEDM nozzle groups. The use of a sister plant's UT data provided a reasonable estimate for the as-built configuration. UT examination at WSES-3 obtained during the Fall 2003 refueling outage will be used to confirm the as-built estimate.
2) The developed models, incorporating a method to account for applied stress distribution variation along the nozzle length, have been shown to be a reasonably realistic but conservative representation of the expected phenomenon. The models are generalized and have the potential to be used at other locations of the nozzles.
3) The fracture mechanics models were shown to be representative of the expected crack and nozzle configurations. A review of the current model results and that from the conventional approach showed that the current model produced higher SIF than the conventional model. Therefore, the current model provides a more accurate and conservative estimate of crack growth.
4) The analyses demonstrate that the UT inspection above the normal blind zone will provide an adequate assurance that the weld will not be compromised in one operating cycle.
5) The plan for the work presented herein, defined additional evaluations that needed to be performed for the determination of an augmented inspection region. However, the deterministic fracture mechanics analyses demonstrated that no additional analyses were required.
6) The additional analysis performed for one location in one nozzle group (49.7° nozzle at the mid-plane location) where the ID surface stress was high shows that the postulated cracks at this location will not compromise the weld for nearly forty (40) years of operation.
7) The regions below the lowest inspection elevation, at other locations, experience lower stresses or have a compression zone. Hence, at elevations below the lowest inspection elevation, a significantly lower potential for crack growth by PWSCC exists. Thus, at these lower locations PWSCC, crack growth is not expected.
8) The ID surface cracks either did not show any potential for crack growth, or the crack growth was well within acceptable limits. Hence, ID surface cracks in a region below the weld are not expected to compromise the weld.

9) The deterministic fracture mechanics analysis demonstrates that the proposed changes to the inspection requirements specified in the NRC Order will still provide an acceptable level of safety and quality commensurate with the NRC Order.

References

1) NRC Order; Issued by letter EA-03-009 addressed to "Holders of Licenses for Operating Pressurized Water Reactors"; dated February 11, 2003.

2) Drawing Number 1564-4086 R1 WSES-3 Design Engineering Drawing files.

3) a: E-mail from R. V. Swain (Entergy) to J. G. Weicks (Entergy); Dated 5/15/2003.

b: E-mail from R. V. Swain to J. G. Weicks; Dated 5/12/2003.

4) EPRI NDE Demonstration Report; "MRP Inspection Demonstration Program – Wesdyne Qualification": Transmitted by e-mail from B. Rassler (EPRI) to K. C. Panther (Entergy); Dated 3/27/2003.

5) a: "PWSCC of Alloy 600 Materials in PWR Primary System Penetrations"; EPRI TR-103696; Electric Power Research Institute, Palo Alto, CA; July 1994.

b: DEI E-Mail containing the Nodal Stress Data for WSES-3 CEDM Analysis; J. Broussard (DEI) to J. S. Brihmadesam (Entergy); E-4162-00-8, Dated 9/2/2003.

c: "BWR Vessel and Internals Project – Evaluation of crack growth in BWR Stainless Steel RPV Internals (BWRVIP-14)"; EPRI TR-105873; Electric Power Research Institute, Palo Alto, CA; March 1996.

d: "BWR Vessel and Internals Project – Evaluation of crack growth in BWR Nickel Base Austenitic Alloys in RPV Internals (BWRVIP-59)"; EPRI TR-108710; Electric Power Research Institute, Palo Alto, CA; December 1998.

6) "Stress Intensity Factor Influence Coefficients for Internal and External Surface Cracks in Cylindrical Vessels"; I. S. Raju and J. C. Newman, Jr.; ASME PVP Volume 58 "Aspects of Fracture Mechanics in Pressure Vessels and Piping"; 1982.

7) "Stress Intensity Factors for Part-Through Surface Cracks in Hollow Cylinders": S. R. Mettu etal; NASA TM-111707; Prepared by Lockheed Engineering & Science Services; Houston, Texas; July 1992.

8) "New Stress Intensity factor and Crack Opening Area Solutions for Through Wall Cracks in Pipes and cylinders": Christine C. France, etal.; ASME PVP Volume 350 "Fatigue and Fracture"; 1997.

9) Axum 7; Data Analysis Products Division, Mathsoft Inc., Seattle, WA; February 1999.

10) a: "Materials reliability Program (MRP) Crack Growth Rates for Evaluating Primary Water Stress Corrosion cracking (PWSCC) of Thick Wall Alloy 600 Material": MRP-55 Revision 1; Electric Power Research Institute; May 2002.

b: "Engineering Report to Support 1.5 percent Power Uprate @ Waterford 3 Steam Electric Station"; ER-WS-ST-0001 Rev. 3; September 2001.

c: "Waterford 3 Extended Power Uprate Report"; (Draft); August 2003.

11) Mathcad – 11; Data Analysis Products Division; Mathsoft Inc.; Seattle WA; November 2002.

12) "Stress Intensity Factors Handbook Volume 1"; Y. Murakami, Editor-in-Chief; Pergamon Press ; 1986; Section 1.3.